Relaxation Property and Stability Analysis of the Quasispecies Models

2009 Commun. Theor. Phys. 52 726

(http://iopscience.iop.org/0253-6102/52/4/33)

Commun. Theor. Phys. (Beijing, China) **52** (2009) pp. 726–734

Vol. 52, No. 4, October 15, 2009

Relaxation Property and Stability Analysis of the Quasispecies Models*

FEGN Xiao-Li,[1,2,†] LI Yu-Xiao,[1] GU Jian-Zhong,[3,4] and ZHUO Yi-Zhong[3]

[1]School of Physical Engineering, Zhengzhou University, Zhengzhou 450052, China

[2]Center for Computational and System Biology, Institute of Biophysics, Chinese Academy of Science, Beijing 100101, China

[3]China Institute of Atomic Energy, P.O. Box 275(18), Beijing 102413, China

[4]Center of Theoretical Nuclear Physics, National Laboratory of Heavy Ion Accelerator of Lanzhou, Lanzhou 730000, China

(Received April 22, 2009)

Abstract *The relaxation property of both Eigen model and Crow–Kimura model with a single peak fitness landscape is studied from phase transition point of view. We first analyze the eigenvalue spectra of the replication mutation matrices. For sufficiently long sequences, the almost crossing point between the largest and second-largest eigenvalues locates the error threshold at which critical slowing down behavior appears. We calculate the critical exponent in the limit of infinite sequence lengths and compare it with the result from numerical curve fittings at sufficiently long sequences. We find that for both models the relaxation time diverges with exponent 1 at the error (mutation) threshold point. Results obtained from both methods agree quite well. From the unlimited correlation length feature, the first order phase transition is further confirmed. Finally with linear stability theory, we show that the two model systems are stable for all ranges of mutation rate. The Eigen model is asymptotically stable in terms of mutant classes, and the Crow–Kimura model is completely stable.*

PACS numbers: 87.10.+e, 87.15.Aa, 87.23.Kg, 89.75.Fb
Key words: relaxation time, critical exponent, error threshold

1 Introduction

Over the past three decades, the quasispecies theory[1−2] and its predicted "error catastrophe" phenomenon have been employed to study the evolution of RNA virus and microbial population due to their high mutation frequency.[3−5] Various evolution models derived from the original Eigen model[1−2] and Crow–Kimura model[6] have been established attempting to explore or explain asexual population evolution. One important quantity is the fitness landscape around which much research has been done from early focusing on simple single peak fitness landscape and static ones[1,7−8] to later choosing more complex and dynamical ones.[9−12] At the same time, the DNA-based genome replication and error repair and recombination effect have also been taken into consideration.[13−18] In recent several years, Krug and Jain[19−21] studied the evolution of maladapted population and traced the evolutionary trajectories on completely rugged fitness landscapes. By approximating the Eigen model to a simply shell model, they found the punctuated behavior of the population fitness change in the limit of strong selection and weak mutation.[19−21] There are lots of experimental work concerning the measure of viral mutation rates and population fitness growth,[22−23] which contributes to modeling population evolution. Incorporating more realistic factors such as interaction between subpopulations and population spatial structure, Nowak *et al.* has extended the quasispecies equation to general replicator-mutator equation.[24] Combining evolutionary game theory, evolutionary graph theory and stochastic effect, the modified quasispecies models have been used to explore and model evolution of tumor or cancer cell population.[25−26]

Unlike biologists concerning the model establishment and application, the physicists and statisticians study new phenomena from physical point of view. Leuthauser[27−28] and Baake, *et al.*[29−31] established an exact correspondence between the two quasispecies models and physical Ising system, respectively. Saakian and Hu solved the two models with general fitness functions comprehensively.[32−34] As phase transition is characterized by three properties: cooperativity, unlimited correlation length, and large scale fluctuations,[35] studying the nature of error threshold transition displayed in the biological models from the three characters is of much importance. Wagner and Baake, *et al.* studied Onsager landscapes and extrapolated that the phase transition for Crow–Kimura model in such case is of second order.[30−31] There are several literatures exploring the error threshold transition for the single peak fitness landscape of Eigen model.[8−9,36] The error threshold transition for the bulk phase appears as a very sharp first order phase transition while it is smoothed by the surface phase with complete wetting.[9] By considering only one mutation per time step which greatly reduces the Eigen model, Gal-

*Supported in part by the National natural Science Foundation of China under Grant No. 10675170 and Major State Basic Research Developing Program under Gant No. 2007CB815003

†E-mail: xlf32@163.com

luccio proved the error threshold phenomenon in the limit of infinite sequence lengths is associated to a first order phase transition. In the sense of analogue of a physical phase transition, the error threshold transition might be of first order.[4,35] However, any calculation of rate constants from sequence, in a similar way as magnetization is related to spin sequences seems inaccessible.[35]

Different from previous work, in this paper we study the error threshold property from phase transition point of view by focusing on the relaxation time which corresponds to the correlation length between inter-sequence layers. The relaxation time is correlated with the eignevalue spectra of the mutation-selection transfer matrix. To facilitate comparison of results between theoretical calculation and numerical curve fittings, the fitness landscape is chosen typically single peaked for both Eigen and Crow–Kimura models. For other fitness landscapes, the same approach is applicable. The paper is organized as follows. In Sec. 2, we generally formulate the two quasispecies models. Comparing with the derivation of the error threshold in the Eigen model, the mutation threshold relation is predicted for the Crow–Kimura model. In Sec. 3, the eigenvalue spectra are analyzed. Then the relaxation time and the critical exponent are calculated both theoretically and numerically. The divergence of relaxation time at the error (mutation) threshold shows the critical slowing-down phenomenon. In Sec. 4, we perform stability analysis of the stationary-state solution. Finally, discussions and conclusions are made in Sec. 5.

2 Quasispecies Dynamics and Error Threshold

The continuous mutation selection dynamics considers the relative frequencies of different genotypes in an infinitely large population. Each genotype (individual or molecule) is represented by a string $\sigma = \{\sigma_1, \sigma_2, \ldots, \sigma_n\}$ of length n, where σ_i can be one of λ values (for DNA or RNA chains, λ =4, but one usually takes λ =2 merely distinguishing purines and pyrimidines). Then the total number of possible genotypes is λ^n. Individual σ replicates with the rate $A(\sigma)$ which represents the fitness of genotype σ. The single peak fitness landscape is defined as such that the master sequence (wild type) denoted by σ^0 has a higher fitness a_0, while all the other sequences have an equal low fitness a_1. In the Eigen model, each site of the sequence has an independent uniform error probability μ during the replication. Then sequence σ can mutate into σ' with a probability $Q_{\sigma'\sigma}$ that is given by

$$Q_{\sigma'\sigma} = \left(\frac{\mu}{\lambda - 1}\right)^{d(\sigma,\sigma')} (1-\mu)^{n-d(\sigma,\sigma')}, \qquad (1)$$

where $d(\sigma, \sigma')$ is the Hamming distance between σ and σ' which counts the number of digits that they differ. Obviously, we have $\sum_{\sigma'} Q_{\sigma'\sigma} = 1$. If we keep the total population number constant, which is equivalent to removal of redundant product of sequences, the mutation selection dynamics for the relative frequency $x_\sigma(t)$ of genotype σ follows

$$\frac{dx_\sigma}{dt} = \sum_{\sigma'} A(\sigma') Q_{\sigma\sigma'} x_{\sigma'} - x_\sigma \sum_{\sigma'} A(\sigma') x_{\sigma'}. \qquad (2)$$

The stationary distribution of the genotypic frequency corresponds to the normalized dominant eigenvector of replication mutation matrix $W(= QA)$. For the master sequence, when the mutation rate is very small, back mutations can be neglected. One then has the stationary frequency of the master sequence σ^0[2]

$$\bar{x}_{\sigma^0} = \frac{a_0/a_1(1-\mu)^n - 1}{a_0/a_1 - 1}, \qquad (3)$$

whose existence is associated with the quasispecies distribution which vanishes at the critical mutation rate μ_c. To guarantee the mutation and selection operate, one must have $n\mu < \ln(a_0/a_1)$, which is the error threshold relation. It imposes an upper bound for the error rate that is needed for the survival of the population.

To obtain the time development of the sequence distribution, one usually deals with the time discrete version, which can be mapped into the two-dimensional Ising system with rows representing molecular sequences at a certain generation. Then the replication mutation matrix is equivalent to the transfer matrix and the molecular distribution at last row of an infinite system corresponds to the stationary state. The phase transition behavior can be perceived by analyzing the eigenvalue spectrum of the transfer matrix. Since the Q matrix is positive and symmetric, for a flat fitness landscape the W matrix is also positive and symmetric, therefore all of its eigenvalues are real. For a general irregular fitness landscape, the W matrix is asymmetric. By means of similarity transformation, it can be changed to a symmetric one.[37] Therefore, the eigenvalues of the W matrix are real. It indicates that no oscillations will exist during evolution.

According to the Perron's theorem, there is a unique largest eigenvalue that is real and positive for the W matrix of finite dimensions, and the largest eigenvalue is an analytic function of the matrix entries. Its associated eigenvector is taken to be positive, which is interpreted as the stationary quasispecies distribution. Therefore, for a finite sequence length, no requirements are satisfied for the occurrence of a phase transition. The only possibility is when n is infinity, which is intractable in practical manipulation. Simulations of the stationary molecular distribution show that the transition from quasispecies distribution to error catastrophe is very sharp at lengths between 100 and 1000.[35] From the biological experimental point of view, the length 100 or even longer is regarded being close to infinity.

Since the replication mutation matrix is of dimensions $2^n \times 2^n$, the eigenvalue spectrum is hardly to obtain for a long sequence. Assuming that sequences which

are equally distant from the master sequence are equally consanguineous in biology, one can group all into $(n+1)$ subset classes according to the Hamming distance from the master sequence. One needs merely to consider the frequency of each mutant class k $(k = 0, 1, \ldots, n)$, that is $y_k = \sum_{\sigma\in k} x_\sigma$. The replication mutation matrix is reduced to a new matrix of $(n+1)$ dimension. The dynamics is formally invariant.

For the Crow–Kimura model, the mutation selection dynamics is slightly simple, which reads

$$\frac{dx_\sigma}{dt} = r(\sigma)x_\sigma + \sum_{\sigma'} m_{\sigma\sigma'}x_{\sigma'} - x_\sigma \sum_{\sigma'} r(\sigma')x_{\sigma'}\,, \qquad (4)$$

where $r(\sigma) = (R)_{\sigma\sigma}$ is the Malthusian fitness which can have an additive shift without changing the stationary distribution. The simple fitness function assumes the independence of replication rates between different sequences. Therefore, the replication matrix R has only diagonal entries. For the single peak fitness landscape, one has $r(\sigma^0) = r_0 > r_1 = r(\sigma')$ for $\sigma' \neq \sigma_0$. And $m_{\sigma\sigma'} = (M)_{\sigma\sigma'}$ is the mutation rate from genotype σ' to σ. It has the following form

$$m_{\sigma\sigma'} = \begin{cases} \mu_0, & \text{if} \quad d(\sigma,\sigma') = 1, \\ -n\mu_0, & \text{if} \quad \sigma = \sigma', \\ 0, & \text{otherwise}, \end{cases} \qquad (5)$$

with μ_0 the mutation rate per unit period of time. Here the replication mutation matrix W corresponds to $(R + M)$.

To predict the mutation threshold on the single peak fitness landscape, we consider the dynamics of the master sequence in terms of mutant classes which by manipulation reads

$$\frac{dy_0}{dt} = (r_0 - r_1)y_0(1 - y_0) - n\mu_0 y_0 + \mu_0 y_1. \qquad (6)$$

Here y_0 and y_1 are the relative frequencies of the master sequence and the mutant class 1. At the stationary state, the left side of the above equation vanishes. We have the relation

$$\bar{y}_0 = \frac{1}{2}\left[\left(1 - \frac{n\mu_0}{r_0 - r_1}\right) + \sqrt{\left(1 - \frac{n\mu_0}{r_0 - r_1}\right)^2 + \frac{4\mu_0\bar{y}_1}{r_0 - r_1}}\right]. \qquad (7)$$

For very small μ_0, $\bar{y}_1$ is very small comparing to $\bar{y}_0$, so the term $(1 - n\mu_0/(r_0 - r_1))$ dominates and $4\mu_0\bar{y}_1/(r_0 - r_1)$ can be neglected. The stationary value $\bar{y}_0$ can be well approximated by

$$\bar{y}_0 \approx 1 - \frac{n\mu_0}{r_0 - r_1}\,. \qquad (8)$$

The survival of σ^0 requires $\mu_0 < (r_0 - r_1)/n$, which appears analogous to the error threshold relation in the Eigen model. This relation, however, is too relaxed to give the correct error threshold. In fact, no matter how large the mutation rate is, $\bar{y}_0$ can be sufficiently close to zero but never approach zero except for $\bar{y}_1 = 0$. With μ_0 increasing from zero, the value $\bar{y}_0$ decreases and the value $\bar{y}_1$ increases. Close to the error threshold, the fraction of $\bar{y}_1$ should not be neglected. Series of simulations of the stationary distribution show that when μ_0 increases to a certain value, $\bar{y}_1$ reaches a fraction that is roughly equal to that of $\bar{y}_0$. When μ_0 increases further, the values of $\bar{y}_0$ and $\bar{y}_1$ decrease almost consistently to zero. One reasonable approximation is that both vanish in the same manner when the mutation rate approaches the critical point. That is $\bar{y}_1 \approx \bar{y}_0$. One then gets the corrected mutation threshold relation

$$\mu_0 < \frac{r_0 - r_1}{n - 1}\,. \qquad (9)$$

The above relation can predict the mutation threshold value fairly well, and prove to be accordant with the critical value obtained from numerical calculations.

Different from the Eigen model, mutations in the Crow–Kimura model occur only between the kin closest sequences. The mutation matrix $M(= (m_{\sigma\sigma'}))$ is symmetric and has the form of Markovian transition matrix. The replication mutation matrix $W(= R + M)$ is real and symmetric. Therefore, it has all real eigenvalues. Then, oscillations will be absent for the evolution dynamics. In fact, the W matrix is a Metzler matrix whose dominant eigenvalue is unique and real and is called the Frobenius eigenvalue. Its associated eigenvector is taken to be positive. Similar to the Eigen model, the non-degeneracy of the dominant eigenvalue for the transfer matrix indicates no phase transition for a finite sequence length.

3 Eigenvalue Spectrum and Relaxation Time

The dynamical behavior at the threshold region and the seeming phase transition feature may become clearer from analysis of the eigenvalue spectrum. Nowak and Schuster[38] studied the spectrum of the classified replication mutation matrix of the Eigen model for short sequences. Successive avoided crossings appear for neighboring eigenvalues with increasing error rate, among which the first avoided crossing accounts for the error threshold transition as shown in Fig. 1.

It seems that all eigenvalues of the reduced replication mutation matrix are real and positive for any error rate. In fact, for a longer sequence with sufficiently large error rates, complex eigenvalues may emerge except for the largest eigenvalue, as is shown in Fig. 2. Since the reduced matrix W' is asymmetric, the largest eigenvalue is guaranteed to be positive only. The complex eigenvalues indicate that above the error threshold, damping oscillations for the mutant class may appear in the evolution process. Indeed, for a finite sequence, the largest eigenvalue is non-degenerate. Calculations for longer sequences show that the gap between the two largest eigenvalues at the threshold region narrows with increasing sequence length. For sufficiently long sequences, the largest and the next largest eigenvalues do intersect at the transition point. In fact, for the case of $n = 100$ or longer, crossing occurs in a tiny scope of the critical region where the slopes of

them are exchanged (Fig. 2). The error threshold can be located with high precision as long as the critical region is subdivided further. It is very similar to the scenario of zero temperature phase transition by level crossing in the Ising model.

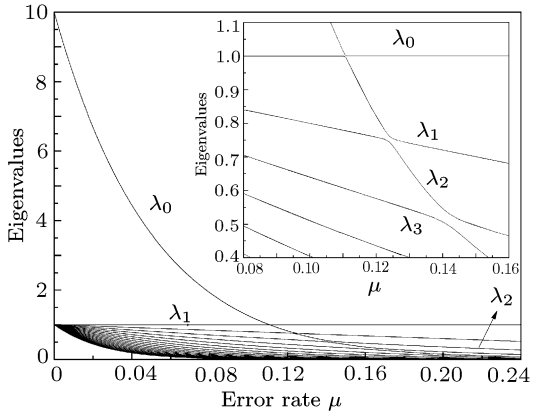

Fig. 1 The spectrum of eigenvalues of the reduced replication mutation matrix as a function of the single-digit error rate μ for the Eigen model with $n = 20$. The fitness landscape is single peaked with $a_0 = 10$ and $a_1 = 1$. The inset figure is the enlarged picture around the error threshold region.

In fact, the logarithm of the dominant eigenvalue of the replication mutation matrix corresponds to the ground state free energy, whose first derivative displays a discontinuity at the error threshold. According to the classification of phase transition, it should generate a first order phase transition in the thermodynamic limit. Thus, as the mutation rate comes closer to the critical point, longer and longer time is needed for the system to equilibrate, which reaches infinity at the exact critical point because of the degeneracy of the dominant eigenvalue. This is the phenomenon of critical slowing down.

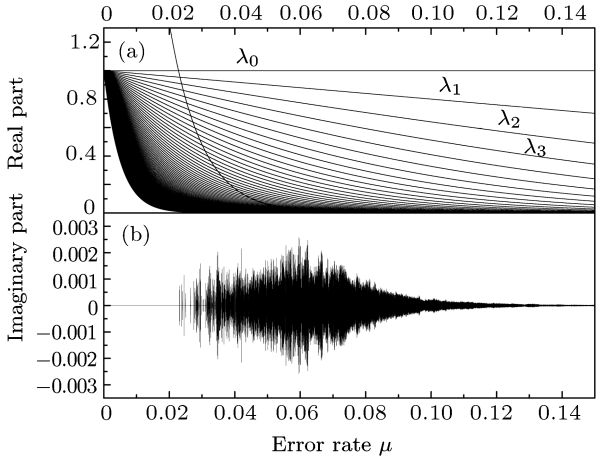

Fig. 2 The spectrum of eigenvalues of the reduced replication mutation matrix as a function of the single-digit error rate μ for the Eigen model with $n = 100$. The fitness landscape is the same as that in Fig. 1.

To find the relaxation behavior especially at the critical point, we treat the replication mutation matrix in terms of mutant classes. The eigenvalues are denoted as $\lambda_0, \lambda_1, \lambda_2, \ldots, \lambda_n$, orderly. By writing the evolution equation in time discrete form, the unnormalized population variable $\mathbf{z}(t)$ reads

$$\mathbf{z}(t) = \mathbf{W}^t \mathbf{z}(0). \tag{10}$$

Here t is a discrete variable. The normalization of $\mathbf{z}(t)$ gives the relative frequency of different mutant classes at generation t. It can be expanded with its eigenvalues λ_i and eigenvectors Ψ_i, that is

$$\mathbf{y}(t) = \frac{\Psi_0 + (\phi_1/\phi_0)(\lambda_1/\lambda_0)^t\Psi_1 + (\phi_2/\phi_0)(\lambda_2/\lambda_0)^t\Psi_2 + \cdots + (\phi_n/\phi_0)(\lambda_n/\lambda_0)^t\Psi_n}{\sum_k[\Psi_{0k} + (\phi_1/\phi_0)(\lambda_1/\lambda_0)^t\Psi_{1k} + (\phi_2/\phi_0)(\lambda_2/\lambda_0)^t\Psi_{2k} + \cdots + (\phi_n/\phi_0)(\lambda_n/\lambda_0)^t\Psi_{nk}]},$$

where the ϕ_i depends on the initial condition. Analogous to the definition of the correlation length, the relaxation time is defined as the inverse logarithm of ratio of the largest to the second largest eigenvalue, i.e.

$$\tau^{-1} = \ln(\lambda_0/\lambda_1).$$

In the thermodynamic limit, the relaxation time should diverge at the critical point. The critical exponent will be calculated below.

Close to the critical point μ_c, the relaxation time τ is expected to vary as ε^ν, where ε is the relative deviation of the critical mutation rate and has $\varepsilon = (\mu_c - \mu)/\mu_c$ for $\mu < \mu_c$, and $\varepsilon = (\mu - \mu_c)/\mu_c$ for $\mu > \mu_c$. In fact, near the critical point, all relevant quantities might have the form $f(\varepsilon) = A\varepsilon^\nu(1 + B\varepsilon^b + \cdots)$ with $b > 0$. If the quantity diverges at the critical point, the $-\nu$ will characterize the divergence exponent. For sufficiently small value of ε, the critical-point exponent can be determined by

$$\nu \equiv \lim_{\varepsilon \to 0} \frac{\ln f(\varepsilon)}{\ln \varepsilon}. \tag{11}$$

Let us first give the theoretical prediction. The largest eigenvalue is in fact the mean fitness of the population at stationary state, so $\lambda_0(\mu) = \langle A \rangle = (a_0 - a_1)\bar{x}_0 + a_1$. The second largest eigenvalue is constant a_1 below the transition point, as is shown in Fig. 2. Combining Eq. (3) and the definition of ε, we have for $(\mu - \mu_c) \to 0^-$

$$\tau(\varepsilon) = \frac{1}{n\ln(1 - \mu_c + \mu_c\varepsilon) + \ln(a_0/a_1)}. \tag{12}$$

Note that $\ln(a_0/a_1) = -n\ln(1 - \mu_c)$. We assume $\varepsilon \to 0$ prior to the thermodynamic limit $n \to \infty$, and then the

critical exponent is calculated as

$$-\nu = -\lim_{n\to\infty}\lim_{\varepsilon\to 0}\frac{\ln\tau(\varepsilon)}{\ln\varepsilon} = -\lim_{n\to\infty}\lim_{\varepsilon\to 0}\frac{-\ln[n\ln(1+(\mu_c/(1-\mu_c))\varepsilon)]}{\ln\varepsilon} = \lim_{n\to\infty}\lim_{\varepsilon\to 0}\frac{\ln[(\mu_c/(1-\mu_c))n\varepsilon)]}{\ln\varepsilon}. \quad (13)$$

We would mention that the limit must be carried out under the condition $n\to\infty$, $\varepsilon\to 0$, and $n\varepsilon\to 0$. So the critical exponent depends on the rate that the multiplicity of n and ε approaches zero. Assume $n\propto\varepsilon^{-\alpha}$ where $0<\alpha<1$, then the above condition is satisfied. Thus, the critical exponent is given by $-\nu=1-\alpha$.

Since in a small region around the critical point, the two largest eigenvalues intersect and change slopes, the critical exponents should be identical for μ approaching μ_c from both sides of the critical point. Realistically, the sequence length at $10^2\sim 10^4$ is very close to infinity, and n is related to ε much weakly. Therefore, α is very close to zero. Experimentally, to obtain the critical exponent, the length n is chosen sufficiently large and constant. Then, the above calculation leads to $-\nu\approx 1$.

To verify our prediction, we resort to numerical simulations. We plot the relaxation time with increasing error rate μ for $n=100$ or longer in Fig. 3(a). The critical exponent can be determined by measuring the slopes of the log-log plots of data τ with ε, which is displayed in Fig. 3(b) and 3(c).

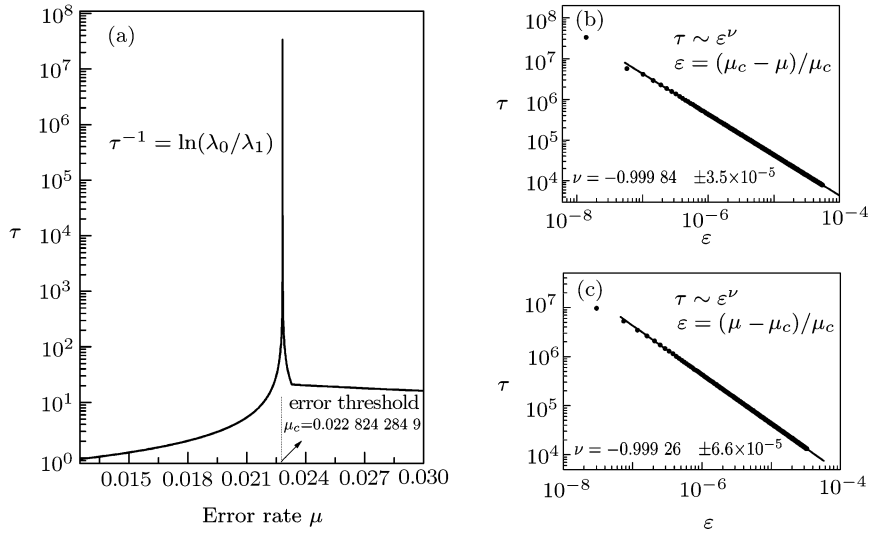

Fig. 3 Relaxation time and the critical exponent for the Eigen model with $n=100$. The fitness landscape is the same as that in Fig. 1. (a) Relaxation time τ with increasing error rate μ. The divergence occurs at the critical point whose value is rounded up to 0.022 824 284 9; (b) and (c) The log-log plot of relaxation time τ with reduced error rate ε from left and right sides of the critical point, respectively. Solid circles represent the numerical data. The straight line fits give the relaxation time exponents $-\nu=0.999\ 84$ and 0.999 26 for $\mu-\mu_c\to 0^-$ and $\mu-\mu_c\to 0^+$, respectively.

One can see that the relaxation time diverges at the threshold whose value is given by $\mu_c=0.022\ 824\ 284\ 9$ at length 100. For a very small region around μ_c, the relaxation time τ changing with reduced error rate ε is fitted, where the coordinates are scaled logarithmically. The slopes of the fitted lines are $-0.999\ 84$ and $-0.999\ 26$ for $\mu-\mu_c\to 0^-$ and $\mu-\mu_c\to 0^+$ respectively. The critical exponents obtained by curve fitting agree quite well with that of the above prediction. It also explains that the sequence length at 100 or longer can give the approximate behavior at the infinite length limit.

For the Crow–Kimura model, we plot the eigenvalues for $n=100$ in Fig. 4. Calculations show that all the eigenvalues are real. Therefore, no oscillations appear for the evolution of mutant classes. For the case of short sequences, no eigenvalues are crossed. For sufficiently long sequences, such as $n=100$ or longer, the largest two eigenvalues do intersect at the threshold point, but the other eigenvalues do not.

Similarly, the relaxation time in the vicinity of the mutation threshold can be derived in terms of ε, which reads

$$\tau(\varepsilon)=\frac{1}{\ln(1+((n-1)\mu_c/r_1)\varepsilon)}. \quad (14)$$

Analogous to (13), the critical exponent can be calculated. Certainly, the limit should be carried out under the same condition $n\to\infty$, $\varepsilon\to 0$, and $n\varepsilon\to 0$. With the same argument, the critical exponent approximately gives $-\nu=1$.

Figure 5(a) gives the relaxation time for $n=100$ with increasing mutation rate for a wide region around the mutation threshold. The mutation threshold value is determined quite precisely. The critical exponents are determined by the slopes of the straight line fits whose values

are -0.9996 and -1.0007 for the mutation rate reaching the critical point from both sides. Also, results by numerical simulations are in good agreement with that of the calculations according to the definition.

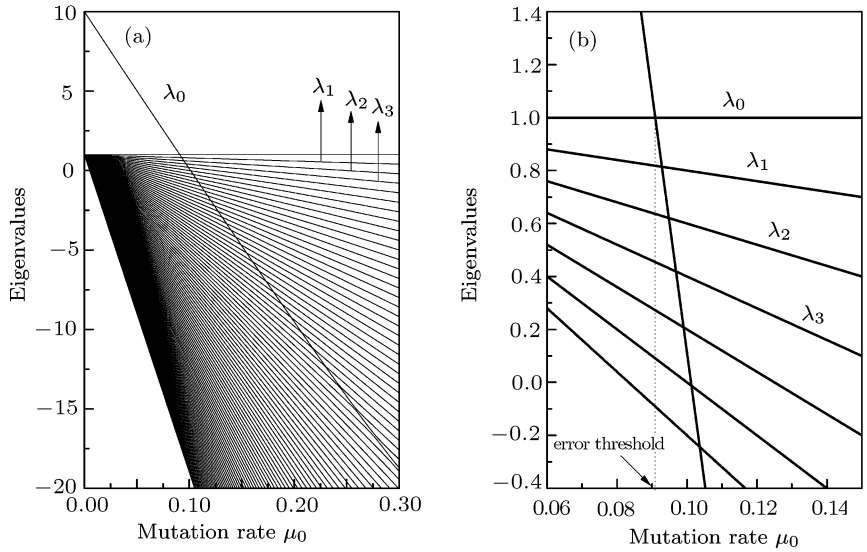

Fig. 4 The spectrum of eigenvalues of the reduced replication mutation matrix as a function of mutation rate μ_0 for the Crow–Kimura model with $n = 100$. The fitness landscape is single peaked with $r_0 = 10$ and $r_1 = 1$. (a) the whole picture of spectrum; (b) local picture of spectrum around the threshold value.

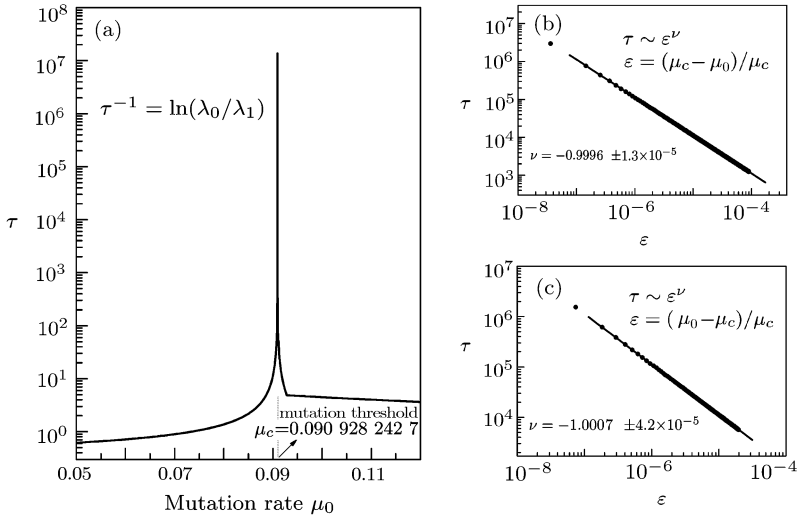

Fig. 5 Relaxation time and the critical exponent for the Crow–Kimura model with $n = 100$. The fitness landscape is the same as that in Fig. 4. (a) Relaxation time τ with increasing mutation rate μ_0. The divergence occurs at the critical point whose value is rounded up to 0.090 928 242 7; (b) and (c) The log-log plot of relaxation time τ with reduced mutation rate ε from left and right sides of the critical point, respectively. Solid circles represent the numerical data. The straight line fits give the relaxation time exponents $-\nu = 0.9996$ and 1.0007 for $\mu_0 - \mu_c \to 0^-$ and $\mu_0 - \mu_c \to 0^+$, respectively.

4 Stability Analysis of Stationary-State Solution

We have known that both the Eigen model and the Crow–Kimura model have a unique steady state solution which serves as the stationary point (or fixed point). However, its stability has not been studied. In this section, we perform the stability analysis for fixed point with linear stability theory.[39] For the Eigen model, we write the equation in terms of mutant classes

$$\frac{dy_i}{dt} = \sum_{k=0}^{n} W'_{ik} y_k - y_i \sum_{k=0}^{n} A(k) y_k = f_i(y_0, y_1, \ldots, y_n)\,. \tag{15}$$

Given the single-digit error rate μ, the steady state solution is written as $\bar{\mathbf{y}} = (\bar{y}_0, \bar{y}_1, \ldots, \bar{y}_n)$. Here we want to know how the system behaves when there is an infinites-

imal perturbation. To examine the stability of solutions in a small neighborhood of the steady state, we expand them about the stationary state

$$y_i = \bar{y}_i + x_i. \tag{16}$$

Let us expand both sides of Eq. (15) into Taylor series, and then we get

$$\begin{aligned}\dot{x}_i = \frac{dx_i}{dt} &= \left(\frac{\partial f_i}{\partial y_0}\right)_{\bar{y}_0,\bar{y}_1,\ldots,\bar{y}_n} x_0 \\ &+ \left(\frac{\partial f_i}{\partial y_1}\right)_{\bar{y}_0,\bar{y}_1,\ldots,\bar{y}_n} x_1 + \cdots \\ &+ \left(\frac{\partial f_i}{\partial y_n}\right)_{\bar{y}_0,\bar{y}_1,\ldots,\bar{y}_n} x_n + o(x^2) \\ &= \sum_{k=0}^{n}\left(\frac{\partial f_i}{\partial y_j}\right)_{\bar{y}_0,\bar{y}_1,\ldots,\bar{y}_n} x_j + o(x^2)\,. \end{aligned} \tag{17}$$

For very small value of x_i, the nonlinear terms can be neglected, then, the above equations reduce to

$$\begin{pmatrix} \dot{x}_0 \\ \dot{x}_1 \\ \vdots \\ \dot{x}_n \end{pmatrix} = \overline{\overline{A}} \begin{pmatrix} x_0 \\ x_1 \\ \vdots \\ x_n \end{pmatrix}, \tag{18}$$

where $\overline{\overline{A}} = (a_{ij})$ is the Jacobian matrix with $a_{ij} = (\partial f_i/\partial y_j)_{\bar{y}_0,\bar{y}_1,\ldots,\bar{y}_n} = W'_{ij} - \bar{A}\delta_{ij} - A(j)y_i$. With a single peak fitness landscape where $a_0 = a$ and $a_1 = 1$, we have

$$\overline{\overline{A}} = \begin{pmatrix} W'_{00} - 2a\bar{y}_0 + \bar{y}_0 - 1 & W'_{01} - \bar{y}_0 & \cdots & W'_{0n} - \bar{y}_0 \\ W'_{10} - a\bar{y}_1 & W'_{11} - \bar{y}_1 - a\bar{y}_0 + \bar{y}_0 - 1 & \cdots & W'_{1n} - \bar{y}_1 \\ W'_{20} - a\bar{y}_2 & W'_{21} - \bar{y}_2 & \cdots & W'_{2n} - \bar{y}_2 \\ \vdots & \vdots & \ddots & \vdots \\ W'_{n0} - a\bar{y}_n & W'_{n1} - \bar{y}_n & \cdots & W'_{nn} - \bar{y}_n - a\bar{y}_0 + \bar{y}_0 - 1 \end{pmatrix}. \tag{19}$$

We next transform Eq. (18) to the form of normal coordinates. Assume the eigenvalues of matrix $\overline{\overline{A}}$ are $\rho_0, \rho_1, \ldots, \rho_n$ and denote $\mathbf{z} = (z_0, z_1, \ldots, z_n)$ the right eigenvector, then, Eq. (18) changes to

$$\begin{pmatrix} \dot{z}_0 \\ \dot{z}_1 \\ \vdots \\ \dot{z}_n \end{pmatrix} = \begin{pmatrix} \rho_0 & 0 & \cdots & 0 \\ 0 & \rho_1 & \cdots & 0 \\ \vdots & \vdots & \ddots & \vdots \\ 0 & 0 & \cdots & \rho_n \end{pmatrix} \begin{pmatrix} z_0 \\ z_1 \\ \vdots \\ z_n \end{pmatrix}. \tag{20}$$

If the initial coordinates' values are $z_i(0)$, the solution in the later time will be $z_i(t) = e^{\rho_i t} z_i(0)$. Generally, the eigenvalues are complex, and the sign of the eigenvalues will govern the stability properties of the system. If the real parts of the eigenvalues are all negative, the perturbation will decay and the solution is stable. If there is at least one positive real part, the perturbation will grow and the solution is unstable. If the real part of one or several eigenvalues happens to be zero, there will be a center manifold for the flow of solution. In this case, at least the second order must be considered to determine the stability of solution.

For the decoupled mutation-selection model, the same method can be applied. The Jacobian matrix has the entries $a_{ij} = (\partial f_i/\partial y_j)_{\bar{y}_0,\bar{y}_1,\ldots,\bar{y}_n} = W'_{ij} - \bar{r}\delta_{ij} - r(j)y_i$. The stability of the stationary-state solution for a single peak fitness landscape can be determined by calculating the eigenvalues of the Jacobian matrix.

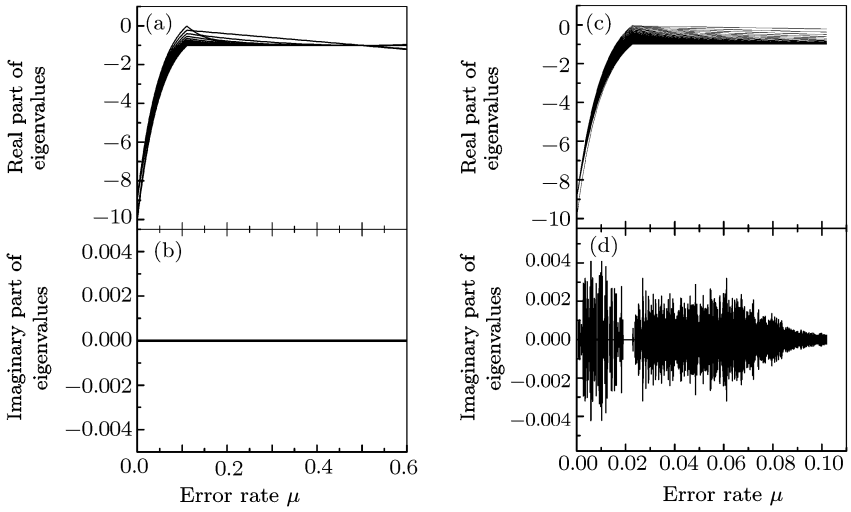

Fig. 6 Eigenvalues of the Jacobian matrix with single-digit error rate for the Eigen model. The fitness landscape is the same as that in Fig. 1. (a) Real part of the eigenvalues with $n = 20$; (b) Imaginary part of eigenvalues with $n = 20$; (c) and (d) eigenvalues with $n = 100$.

In the calculations, we choose the molecular sequence length $n = 20$ and $n = 100$. By using linear stability theory, we perform the local stability analysis at the steady state. For different replication error rates, we compute the eigenvalues of Jacobian matrix. The numerical results are displayed in Fig. 6.

It can be seen that for the Eigen model with a short sequence length, all the eigenvalues of the Jacobian matrix are real and negative, which implies the steady-state solution is stable. A pronounced transition occurs at the error threshold where the largest eigenvalue is close to zero. For longer sequence such as $n = 100$, several complex eigenvalues emerge, but the real parts of them are negative, indicating that the system is asymptotically stable. At the threshold, the largest eigenvalue is real and negative for finite n. Only for $n \to \infty$ does it reach zero, which implies a diverging relaxation time for the system decaying back to the equilibrium.

For the Crow–Kimura model, results are shown in Fig. 7. In terms of the classified mutant classes, all the eigenvalues are negative and real, therefore, the system is completely stable.

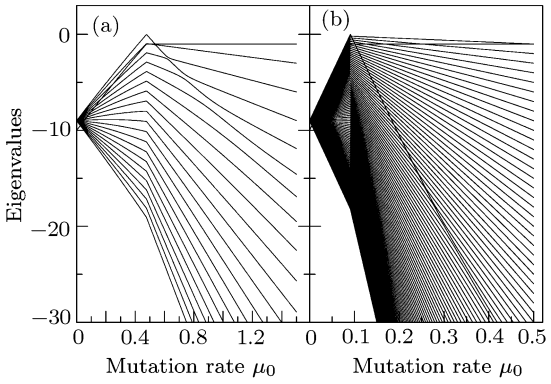

Fig. 7 Eigenvalues of the Jacobian matrix with mutation rate per site for the Crow–Kimura model. The fitness landscape is the same as that in Fig. 4. (a) $n = 20$; (b) $n = 100$.

5 Discussion and Conclusions

The location of the error threshold and the nature of error threshold transition depend on the choice of fitness landscape. Usually, the location of the error threshold can not be exactly determined for a finite sequence length, which can be realized either by theoretical approximation or relying on the thermodynamic limit. In our work, the fitness and the single digit error rate (or mutation rate per site) for both quasispecies models are treated as intensive variables and the error (mutation) threshold relation is obtained under reasonable approximations or assumptions. In fact, in the case of single peak fitness landscape, variable scaling does not change the critical behavior. Franz and Peliti[29] studied the error threshold property by taking the sequence length to infinity while keeping the single-point mutation rate constant which is equivalent to increasing selection superiority exponentially. The transition at the threshold is still of first order. For other complicated fitness landscapes such as Onsager landscape and mean-field landscape where the fitness and mutation per genome are treated as extensive variables,[31] the thermodynamic limit is employed to investigate the critical behavior.

Different from their work, we mainly study the relaxation property especially for mutation rate close to the critical point for both Eigen and Crow–Kimura models. Though the two models are different in mutation mechanisms, they share very similar relaxation behavior. Both replication-mutation matrices have all real eigenvalue spectra with respect to the genotypes. With respect to mutant classes, however, damping oscillations may appear for Eigen model with large error rates. In fact, in the weak mutation limit, only the one point mutation is important, which reduces the dynamical equations of Eigen model to a form similar to that of Crow–Kimura model. At the critical point, Galluccio[8] deduced that the typical amplitude of the quasispecies around the master sequence which is the localization length diverges with exponent 1 for Eigen model. His work proved the property of cooperativity (or long range order) at the critical point. In a different way, we calculate the relaxation time which in fact corresponds to the correlation length of sequence systems. Interestingly enough, for both models at the error threshold, the relaxation time diverges with exponent 1. The critical exponents from theoretical prediction and the numerical curve fittings agree quite well. Thus the unlimited correlation length (or critical slowing down behavior) for infinite sequence lengths at the error threshold point is confirmed.

In addition to the similar relaxation property, the stabilities of the steady state solution for both models are similar too. With linear stability analysis, we show that for any error rate (mutation rate), both equilibrium solutions are stable against small perturbations. The Eigen model is stable, and the solution with respect to the mutant class spirals towards the steady state, thus the stationary state solution is a stable spiral. The Crow–Kimura model is stable, and a solution deviating equilibrium will decay exponentially back to the steady state, thus the stationary state solution is a stable node. While our previous study with the single peak Gaussian distributed fitness landscapes[12] shows the error threshold is stable against small fitness fluctuations, the equilibrium at the error threshold under the influence of small perturbations is stable from the dynamical point of view. Thus, we conclude that both the error threshold and the steady-state solution at it are stable under weak perturbations for both models.

In conclusion, we studied the relaxation property and performed stability analysis with the single peak fitness landscape for both Eigen and Crow–Kimura models. Comparing to Eigen model, the mutation threshold relation for Crow–Kimura model with a single peak fitness landscape is predicted. From phase transition point of view, we find the relaxation time at the threshold point diverges with exponent 1, which reveal the critical slowing down phenomenon. Thus the unlimited correlation length further verifies the phase transition property. In addition, by means of linear stability analysis, the stationary-state solution of both models proves to be stable.

Acknowledgment

We thank Professors Hans A. Weidenmüller and O. Bohigas for helpful discussions and suggestions.

References

[1] M. Eigen, Naturwissenchaften **58** (1971) 465.

[2] M. Eigen, J. McCaskill, and P. Schuster, Adv. Chem. Phys. **75** (1989) 149.

[3] S. Crotty, C.E. Cameron, and R. Andino, Proc. Natl. Acad. Sci. USA **98** (2001) 6895.

[4] M. Eigen, Proc. Natl. Acad. Sci. USA **99** (2002) 13374.

[5] C.K. Biebricher and M. Eigen, Virus Res. **107** (2005) 117.

[6] J.F. Crow and M. Kimura, *An Introduction to Population Genetics Theory*, Harper and Row, New York (1970).

[7] J. Swetina and P. Schuster, Biol. Chem. **16** (1982) 329.

[8] S. Gaulluccio, Phys. Rev. E **56** (1997) 4526.

[9] P. Tarazona, Phys. Rev. A **45** (1992) 6038.

[10] C.O. Wilke, *et al.*, Phys. Rep. **349** (2001) 395.

[11] M. Nilsson and N. Snoad, Phys. Rev. E **65** (2002) 031901.

[12] X. Feng, Y. Li, J. Gu, *et al.*, J. Theor. Biol. **246** (2007) 28.

[13] E. Tannenbaum, E.J. Deeds, and E.I. Shaknovich, Phys. Rev. E **69** (2004) 061916.

[14] E. Tannenbaum and E.I. Shaknovich, Phys. Rev. E **69** (2004) 011902.

[15] E. Tannenbaum, J.L. Sherley, and E.I. Shaknovich, Phys. Rev. E **70** (2004) 061915.

[16] E. Tannenbaum, E. Deeds, and E.I. Shaknovich, Phys. Rev. Lett. **91** (2003) 138105.

[17] Y. Brumer and E. I. Shakhnovich, Phys. Rev. E **70** (2004) 061912.

[18] J.M. Park and M.W. Deem, Phys. Rev. Lett. **98** (2007) 058101.

[19] J. Krug and C. Karl, Phys. A **318** (2003) 137.

[20] K. Jain and J. Krug, J. Stat. Mech. (2005) P04008.

[21] K. Jain, Phys. Rev. E **76** (2007) 031922.

[22] I.S. Novella, E.A. Durte, S.F. Elena, *et al.*, Proc. Natl. Acad. Sci. USA **92** (1995) 5841.

[23] J.W. Drake and J.J. Holland, Proc. Natl. Acad. Sci. USA **96** (1999) 13910.

[24] M.A. Nowak, *Evolutionary Dynamics: Exploring the Equations of Life*, Belknap Press, Harvard University (2006).

[25] R.V. Solé, Eur. Phys. J. B **35** (2003) 117.

[26] R.V. Solé and T.S. Diesboeck, J. Theor. Biol. **228** (2004) 47.

[27] I. Leuthäusser, J. Chem. Phys. **84** (1986) 1884.

[28] I. Leuthäusser, J. Stat. Phys. **48** (1987) 343.

[29] E. Baake, M. Baake, and H. Wagner, Phys. Rev. Lett. **78** (1997) 559.

[30] H. Wagner, E. Baake, and T. Gerisch, J. Stat. Phys. **92** (1998) 1017.

[31] E. Baake and H. Wagner, Genet. Res. Camb. **78** (2001) 93.

[32] D.B. Saakian and C.K. Hu, Phys. Rev. E **69** (2004) 021913; D.B. Saakian and C.K. Hu, Phys. Rev. E **69** (2004) 046121.

[33] D.B. Saakian, C.K. Hu, and H. Khachatryan, Phys. Rev. E **70** (2004) 041908.

[34] D.B. Saakian and C.K. Hu, Proc. Natl. Acad. Sci. USA **103** (2006) 4935.

[35] M. Eigen, Biophys. Chem. **85** (2000) 101.

[36] S. Franz and L. Peliti, J. Phys. A: Math. Gen. **30** (1997) 4481.

[37] D.S. Rumschitzki, J. Math. Biol. **24** (1987) 667-680.

[38] M. Nowak and P. Schuster, J. Theor. Biol. **137** (1989) 375.

[39] L.E. Reichl, *A Modern Course in Statistical Physics*, 2nd ed., John Wiley and Sons, Inc., New York (1998).